The distorted-wave impulse approximation for electron capture into excited states

Yiu Hong Ng and Jim McCann

Atomic and Molecular Physics Group †, Department of Physics, University of Durham, Durham DH1 3LE, UK.

Abstract. Total cross sections for electron capture are calculated for collisions of fast protons and α–particles with atomic hydrogen. The distorted-wave impulse approximation is applied over the energy range 10–1500 keV/u. State-selective results are given for the $1s$, $2s$ and $2p$ levels. Both the *post* and *prior* forms of the model are calculated and compared with results from other theories and experimental measurements. In general the model performs very well in comparison with experiment over this energy range though discrepancies arise at lower energies.

1. Introduction

The study of the interaction between atomic hydrogen and fast ions has an important role in the physics of fusion plasmas (Gilbody 1995). It is significant also in other areas of research such as the study of stellar atmospheres (Janev *et al* 1987) and the physics of proton aurorae (Van Zyl 1993). An essential requirement for the study of these complex phenomena is the availability of accurate data for a wide variety of fundamental ion-atom collision processes. Given that the velocity range is such that we can consider the nuclear motion as classical and solve the time-dependent equation of motion for the electrons, one might suppose that simulations of these processes would be rather simple. However this is not the case, and the theory behind this problem remains an area of active investigation (Bransden and McDowell 1993). While different strategies have been applied to problems of this nature, the most common approach relies on basis function expansions (Fritsch and Lin 1991, Kuang and Lin 1996, McLaughlin *et al* 1997). This and other methods, including the the direct solution of the partial-differential equation, have been reviewed comprehensively by Bransden and McDowell (1993).

While the basis function method has a well-founded popularity, it does have some drawbacks. Firstly, it can be computationally expensive when excited-state coupling

† Research URL: http://www.dur.ac.uk/∼dph0www1

is involved. Moreover the choice of basis set is problematic; one cannot always rely on the use of larger basis sets to produce better data. Kuang and Lin (1996) indicate some of the spurious effects that can arise if the size and type of a basis set are not appropriate. In spite of these caveats, it is fair to say that recent large-scale calculations of this type have given excellent agreement with experimental data over the appropriate energy range (McLaughlin *et al* 1997). There exist limitations to the method because it is primarily designed for strong diabatic coupling between bound states which are nondegenerate. It tends to work less well for higher energies at which ionization (continuum coupling) is prevalent, and when mixing with nearly degenerate states takes place. While significant advances have been made in the use of pseudostates to simulate such coupling (Slim and Ermolaev 1994, McLaughlin *et al* 1997) the implementation of the method requires access to high-performance computers. An innovation marrying bound and continuum states has been developed by Brown and Crothers (1994, 1996a, 1996b) and includes continuum coupling explicitly in the wavefunctions. This is known as the symmetrized variational continuum distorted-wave (SVCDW) method and it gives excellent agreement with experimental data for electron capture, excitation and ionization over the intermediate energy region.

Our paper is concerned with fundamental charge exchange processes, namely those occurring between hydrogen atoms and fast protons or α–particles. Charge exchange poses theoretical difficulties in that one requires an accurate description of the electron dynamics around both the target and projectile. Often a large two-centre basis function expansion is the prescription for achieving this aim, or a restricted optimized expansion (Brown and Crothers 1994). Considering alternatives to these approaches, the fact that charge exchange rapidly decreases in importance as the energy is increased means that one can often use perturbation theory at high energies to obtain reliable predictions (Belkić *et al* 1979). This also has the advantage in being easy to calculate even with modest computational resources. However, refinements of perturbation theory, including second-Born type corrections, are much more difficult to compute and often do not improve the agreement with experiment (Bransden and McDowell 1993). This paper investigates the effectiveness of extending one such *high-energy* approximation into an *intermediate* energy regime. Here we understand the term *intermediate energy* to refer to the range 10-200 keV/u, and this is the range of greatest interest for beam injection techniques used in fusion science (Gilbody 1995). The method we adopt, the distorted-wave impulse approximation (DWIA), though based upon perturbation theory can account for high-order potential scattering from both centres. However the theory is not of the close-coupling type and thus in its present form cannot describe strong intrashell (Stark) mixing or backcoupling (McCann 1992).

The DWIA was formulated (Miraglia 1982) as an improvement upon the conventional plane-wave impulse approximation (PWIA) for electron capture in ion-atom collisions.

The PWIA is designed to work for collisions in which the collision is fast in terms of the atomic time-scales (projectile or target). The validity for the impulse approximation depends upon the collision time being much shorter than some characteristic orbital period of the electron bound state. This prerequisite comes from treating the weaker interacting nucleus as a spectator particle. If the collision is sufficiently fast on the atomic time-scale of this particle then the spectator particle cannot interact strongly with the electron during the transition. Its role is confined to describing the electronic state before or after the supposed three-body interaction in terms of binding the electron and providing it with a momentum distribution in the bound state. This establishes a loose validity criterion for the approximation that the collision time should be shorter than the internal interaction time, or in other words, the atomic orbital period. In applications the impulse approximation was found to be very effective in reproducing a large variety of experimental data for very fast collisions (Jakubassa-Amundsen and Amundsen 1980). However the inherent asymmetry of the method leads to *post* and *prior* forms of the transition amplitude; in general these do not agree well. The two versions of the approximation converge at high energies, but strongly diverge at intermediate and low energies. On the other hand the DWIA seems to be better suited to both symmetric and asymmetric collisions. While we find that there is still a *post-prior* discrepancy, it is very much less than that which arises from using the PWIA. We employ this model to investigate the following collision processes

$$\mathrm{H}^+ + \mathrm{H}(1s) \rightarrow \mathrm{H}(1s, 2s, 2p) + \mathrm{H}^+ \tag{1}$$

and

$$\mathrm{He}^{2+} + \mathrm{H}(1s) \rightarrow \mathrm{He}^+(1s, 2s, 2p) + \mathrm{H}^+. \tag{2}$$

These are ideal processes to test any theory because the atomic structure is trivial. Also the absence of screening effects allows us to write continuum states in terms of Coulomb functions. For this reason the evaluation of matrix elements is straightforward.

2. Method

In this three-body re-arrangement reaction, we have a bare projectile nucleus of charge Z_P travelling at a velocity $\boldsymbol{v}$ relative to the target atom which has nuclear charge Z_T. The position of the electron in question, with respect to the target and projectile nuclei, is defined to be $\boldsymbol{r}_T$ and $\boldsymbol{r}_P$, respectively. The initial and final atomic energies of the electron are denoted by E_T and E_P, corresponding to the target and projectile state electron wavefunctions Φ_i and Φ_f. The momentum-space representations of these states are labelled as $\tilde{\Phi}_i$ and $\tilde{\Phi}_f$ in this paper.

The definitions of *post* and *prior* can lead to confusion so let us clarify their meanings. We use the standard convention that *post* refers to using the impulse approximation in

the initial channel for the interaction between the projectile ion and target atom. In order to calculate the *prior* form, a separate program must be written.

$$\text{DWIA}(post) \quad P(\text{PWIA}) + (e^-, T) \rightarrow (P, e^-) + T(\text{CDW}) \tag{3}$$

$$\text{DWIA}(prior) \quad P(\text{CDW}) + (e^-, T) \rightarrow (P, e^-) + T(\text{PWIA}) \tag{4}$$

In the *prior* form, the DWIA transition amplitude $a_{fi}^{(-)}(\boldsymbol{b})$ for a given impact parameter $\boldsymbol{b}$ consists of a continuum distorted-wave $\xi_{CDW}^{(+)}$ in the entrance channel and a distorted-wave $\chi_{IA}^{(-)}$ from the PWIA in the exit channel:

$$a_{fi}^{(-)}(\boldsymbol{b}) = -i \int_{-\infty}^{\infty} \mathrm{d}t \, \langle \chi_{IA}^{(-)} \mid H - i\partial_t \mid \xi_{CDW}^{(+)} \rangle \tag{5}$$

The expression in momentum-space (McCann 1992) in the *prior* form is:

$$\tilde{a}_{fi}^{(-)}(\boldsymbol{\eta}) = (2\pi)^{-5/2} v^{-1} i N(a_P) \int \mathrm{d}\boldsymbol{k} \; N(a_T) \; \tilde{\Phi}_f^*(\boldsymbol{k} - \boldsymbol{v}) \; \boldsymbol{c} \cdot \boldsymbol{d} \tag{6}$$

$$\boldsymbol{c} = \int \mathrm{d}\boldsymbol{r}_T \; \exp(i\boldsymbol{\mu} \cdot \boldsymbol{r}_T) \; {}_1F_1 \left[ia_T; 1; i(kr_T + \boldsymbol{k} \cdot \boldsymbol{r}_T)\right] \nabla_{r_T} \Phi_i(\boldsymbol{r}_T) \tag{7}$$

$$\boldsymbol{d} = \int \mathrm{d}\boldsymbol{r}_P \; \exp(i\boldsymbol{\omega} \cdot \boldsymbol{r}_P) \; \nabla_{r_P} \, {}_1F_1[ia_P; 1; i(vr_P + \boldsymbol{v} \cdot \boldsymbol{r}_P)] \tag{8}$$

with the momentum transfer vector $\boldsymbol{\mu} = -\boldsymbol{\eta} + (\Delta E/v^2 - \frac{1}{2})\boldsymbol{v}$, $a_T = Z_T/k$, $a_P = Z_P/v$ and $\boldsymbol{\omega} = -\boldsymbol{\mu} - \boldsymbol{k}$, the electron momentum being $\boldsymbol{k}$. The transverse impulse is denoted by $\boldsymbol{\eta}$. The normalization factor $N(x)$ is defined by $N(x) = \exp(\pi x/2) \; \Gamma(1 - ix)$, and $\Delta E = E_P - E_T$. The *post* form of the transition amplitude is:

$$\tilde{a}_{fi}^{(+)}(\boldsymbol{\eta}) = (2\pi)^{-5/2} v^{-1} i N(a'_T) \int \mathrm{d}\boldsymbol{k} \; N(a'_P) \; \tilde{\Phi}_i(\boldsymbol{k} + \boldsymbol{v}) \; \boldsymbol{c'} \cdot \boldsymbol{d'} \tag{9}$$

$$\boldsymbol{c'} = \int \mathrm{d}\boldsymbol{r}_P \; \exp(i\boldsymbol{\mu'} \cdot \boldsymbol{r}_P) \; {}_1F_1 \left[ia'_P; 1; i(kr_P - \boldsymbol{k} \cdot \boldsymbol{r}_P)\right] \nabla_{r_P} \Phi_f^*(\boldsymbol{r}_P) \tag{10}$$

$$\boldsymbol{d'} = \int \mathrm{d}\boldsymbol{r}_T \; \exp(i\boldsymbol{\omega'} \cdot \boldsymbol{r}_T) \; \nabla_{r_T} \, {}_1F_1[ia'_T; 1; i(vr_T + \boldsymbol{v} \cdot \boldsymbol{r}_T)] \tag{11}$$

Here the momentum transfer vector $\boldsymbol{\mu'} = \boldsymbol{\eta} - (\Delta E/v^2 + \frac{1}{2})\boldsymbol{v}$, $a'_T = Z_T/v$, $a'_P = Z_P/k$ and $\boldsymbol{\omega'} = -\boldsymbol{\mu'} + \boldsymbol{k}$.

For the purposes of our calculation we have considered transitions between excited target states and the projectile ground state. One can always relate the data obtained to the inverse reaction using the principle of detailed balance and time-reversal symmetry, *i.e.* cross sections for the processes (1) and (2) can be elicited by looking at their time-reversed counterparts:

$$\mathrm{H}^+ + \mathrm{H}(1s, 2s, 2p) \rightarrow \mathrm{H}(1s) + \mathrm{H}^+ \tag{12}$$

and

$$\mathrm{H}^+ + \mathrm{He}^+(1s, 2s, 2p) \rightarrow \mathrm{He}^{2+} + \mathrm{H}(1s). \tag{13}$$

In our calculations we have therefore explicitly considered electron capture *into* the $1s$ state from the $1s$, $2s$ and $2p_{x,y,z}$ states. From now on, we will discuss calculations in terms of the *prior* form only, for the sake of convenience.

2.1. $2s$-$1s$ *transition*

Previous work using the DWIA (Gravielle and Miraglia 1988) dealt with electron capture from the K shell, specifically $1s$-$1s$ electron transfer. It was noted (McCann 1992) that the evaluation of the azimuthal integral, with the polar axis lying along the momentum transfer vector $\boldsymbol{\mu}$, generates an Appell function F_1 (Appell and Kampé de Feriet 1926) which is a hypergeometric function of two variables. Its many linear transformations and analytic continuations (Olsson 1964) can be used to evaluate this function. Nevertheless it remains a major obstacle to efficient and accurate computation of the capture cross section.

For the case of $2s$-$1s$ electron transfer, it can easily be shown using parametric differentiation that the spatial integrals, (7) and (8), over $\boldsymbol{r}_T$ and $\boldsymbol{r}_P$ simplify in a manner very similar to that found in the $1s$-$1s$ symmetric transfer calculation (McCann 1992). Using spherical coordinates for the $\boldsymbol{k}$–integral in (6), we denote the angles between $\boldsymbol{\mu}$ and $\boldsymbol{k}$, and that between $\boldsymbol{\mu}$ and $\boldsymbol{v}$ by $\theta_{\mu k}$ and $\theta_{\mu v}$. Taking the angle between these two planes as ϕ, we then encounter the following term:

$$\int_0^{2\pi} \mathrm{d}\phi\ (A + B\cos\phi)^{-2}(C + D\cos\phi)^{-1-ia_P} = 2\pi(A+B)^{-2}(C+D)^{-1-ia_P} \times F_1(\tfrac{1}{2}; 2, 1+ia_P; 1; x_1, x_2) \tag{14}$$

with $x_1 = 2B/(A+B)$ and $x_2 = 2D/(C+D)$. The quantities A, B, C and D have the definitions:

$$\begin{aligned} A &= Z_P^2 + v^2 + k^2 - 2vk\cos\theta_{\mu k}\cos\theta_{\mu v} \\ B &= 2vk\sin\theta_{\mu k}\sin\theta_{\mu v} \\ C &= -\Delta E + v^2/2 - vk\cos\theta_{\mu k}\cos\theta_{\mu v} \\ D &= vk\sin\theta_{\mu k}\sin\theta_{\mu v} \end{aligned} \tag{15}$$

2.2. $2p$-$1s$ *transition*

The lack of spherical symmetry for the $2p$ sub-states means that the choice of the axis of quantization is important (Coleman and Trelease 1968). Using the momentum transfer vector $\boldsymbol{\mu}$ as the polar axis simplifies calculations and the change to the laboratory frame of reference requires a simple rotation transformation.

A different line of approach takes advantage of parametric differentiation. We can consider the spherical harmonics in their real form:

$$\Phi_{2p_j}(\boldsymbol{r}_T) = \tfrac{1}{4} Z_T^{5/2} (2\pi)^{-1/2} \exp(-\lambda_T r_T)\ r_{Tj} \tag{16}$$

where $\lambda_T = \frac{1}{2} Z_T$ and $j \in \{x, y, z\}$. In evaluating (7), integration by parts gives:

$$\boldsymbol{c} = \boldsymbol{I_1} + \boldsymbol{I_2} \tag{17}$$

Table 1. Cross sections σ_{nl} (10^{-17}cm^2) of electron capture for proton-hydrogen collisions at energy E keV: $1s$ to nl transition. The integer in parenthesis indicates the power of ten by which the number has to be multiplied.

E(keV)		125	250	500	750	1000	1500
σ_{1s}	DWIA	2.45(-1)	1.35(-2)	4.83(-4)	5.97(-5)	1.30(-5)	1.43(-6)
	CDW	2.70(-1)	1.38(-2)	4.83(-4)	5.96(-5)	1.29(-5)	1.43(-6)
σ_{2s}	DWIA$_{post}$	4.68(-2)	2.19(-3)	6.98(-5)	8.23(-6)	1.74(-6)	1.87(-7)
	DWIA$_{prior}$	4.50(-2)	2.20(-3)	7.02(-5)	8.28(-6)	1.75(-6)	1.88(-7)
	CDW	5.05(-2)	2.26(-3)	7.13(-5)	8.43(-6)	1.79(-6)	1.93(-7)
σ_{2p}	DWIA$_{post}$	9.89(-3)	2.65(-4)	4.93(-6)	4.42(-7)	7.78(-8)	6.54(-9)
	DWIA$_{prior}$	1.29(-2)	3.76(-4)	7.38(-6)	6.60(-7)	1.15(-7)	9.67(-9)
	CDW	1.54(-2)	4.83(-4)	1.01(-5)	9.53(-7)	1.74(-7)	1.58(-8)

$$\boldsymbol{I_1} = -\int \mathrm{d}\boldsymbol{r}_T \ \exp(i\boldsymbol{\mu}\cdot\boldsymbol{r}_T)\ \Phi_i(\boldsymbol{r}_T)\ \nabla_{r_T}\ {}_1F_1[ia_T;1;i(kr_T+\boldsymbol{k}\cdot\boldsymbol{r}_T)] \tag{18}$$

$$\boldsymbol{I_2} = -i\boldsymbol{\mu}\int \mathrm{d}\boldsymbol{r}_T \ \exp(i\boldsymbol{\mu}\cdot\boldsymbol{r}_T)\ {}_1F_1[ia_T;1;i(kr_T+\boldsymbol{k}\cdot\boldsymbol{r}_T)] \tag{19}$$

The integral $\boldsymbol{I_1}$ is further simplified by writing it as:

$$\begin{aligned}
\boldsymbol{I_1} &= -q\frac{\partial}{\partial \boldsymbol{q}}\int \mathrm{d}\boldsymbol{r}_T\ \frac{\exp(i\boldsymbol{\mu}\cdot\boldsymbol{r}_T)}{r_T}\Phi_i(\boldsymbol{r}_T){}_1F_1[ia_T;1;i(qr_T+\boldsymbol{q}\cdot\boldsymbol{r}_T)]\Big|_{\boldsymbol{q}=\boldsymbol{k}} \\
&= \tfrac{1}{4}{Z_T}^{5/2}(2\pi)^{-1/2}iq\frac{\partial}{\partial \boldsymbol{q}}\frac{\partial}{\partial \mu_j}\int \mathrm{d}\boldsymbol{r_T}\ \frac{\exp(-\lambda_T r_T+i\boldsymbol{\mu}\cdot\boldsymbol{r_T})}{r_T} \\
&\quad \times {}_1F_1[ia_T;1;i(qr_T+\boldsymbol{q}\cdot\boldsymbol{r_T})]\Big|_{\boldsymbol{q}=\boldsymbol{k}} \\
&= \tfrac{1}{4}{Z_T}^{5/2}(2\pi)^{-1/2}iq\frac{\partial}{\partial \boldsymbol{q}}\frac{\partial}{\partial \mu_j}\Big[\frac{2\pi\alpha^{ia_T-1}}{(\alpha+\beta)^{ia_T}}\Big]\Big|_{\boldsymbol{q}=\boldsymbol{k}}
\end{aligned} \tag{20}$$

where $\alpha = \frac{1}{2}({\lambda_T}^2+\mu^2)$, $\beta = \boldsymbol{\mu}\cdot\boldsymbol{q} - i\lambda_T\ q$, and $\partial/\partial\mu_j$ calls for partial differentiation with respect to the j component of $\boldsymbol{\mu}$, $j\in\{x,y,z\}$. The momentum transfer vector $\boldsymbol{\mu}$ consists of two mutually orthogonal components, with one running parallel to the direction of travel $\hat{\boldsymbol{v}}$ of the incoming projectile which we can take as the z-axis. The transverse component is $-\boldsymbol{\eta}$ and this lies within the xy-plane. It is then convenient to let $\boldsymbol{\eta}$ lie along the $x(y)$-axis with the result that capture from the $2p_{y(x)}$ state is parity forbidden.

Employing the same method, the expression (19) can be shown to be given by:

$$\boldsymbol{I_2} = \tfrac{1}{4}{Z_T}^{5/2}(2\pi)^{-1/2}\boldsymbol{\mu}\frac{\partial}{\partial\lambda_T}\frac{\partial}{\partial\mu_j}\Big[\frac{2\pi\alpha^{ia_T-1}}{(\alpha+\beta)^{ia_T}}\Big] \tag{21}$$

For electron capture from the $2p$ states, the azimuthal integral of (6) has the form:

$$J = \int_0^{2\pi} \mathrm{d}\phi \, (A' + B' \cos\phi)^{-2} \, (C' + D' \cos\phi)^{-1-ia_P} \, (E' + F' \cos\phi) \tag{22}$$

Like those of (15), the quantities A', B', C', D', E' and F' depend upon $\boldsymbol{\eta}$, $\boldsymbol{k}$ and the polar angle between $\boldsymbol{k}$ and $\boldsymbol{\mu}$, but are much more complicated; we do not quote the details.

Parametric differentiation transforms (22) into an expression containing derivatives of the more familiar Appell functions F_1.

$$\begin{aligned} J &= -(E' \frac{\partial}{\partial A'} + F' \frac{\partial}{\partial B'}) \int_0^{2\pi} \mathrm{d}\phi \, (A' + B' \cos\phi)^{-1} \, (C' + D' \cos\phi)^{-1-ia_P} \\ &= -(E' \frac{\partial}{\partial A'} + F' \frac{\partial}{\partial B'}) \{ 2\pi (A' + B')^{-1} (C' + D')^{-1-ia_P} \\ &\quad \times F_1(\tfrac{1}{2}; 1, 1 + ia_P; 1; x_1, x_2) \} \end{aligned} \tag{23}$$

Since

$$\partial_{x_1} F_1(a; b_1, b_2; c; x_1, x_2) = \frac{a b_1}{c} F_1(a + 1; b_1 + 1, b_2; c + 1; x_1, x_2) \tag{24}$$

we therefore have:

$$\begin{aligned} J = -2\pi (A' + B')^{-3} (C' + D')^{-1-ia_P} \{ & F_1(\tfrac{3}{2}; 2, 1 + ia_P; 2; x_1, x_2) \, (A'F' - B'E') \\ & - F_1(\tfrac{1}{2}; 1, 1 + ia_P; 1; x_1, x_2) \, (A' + B')(E' + F') \} \end{aligned} \tag{25}$$

As with $1s$-$1s$ electron capture, the corresponding $2s$-$1s$ and $2p$-$1s$ transition amplitudes possess two singularities, at $C \pm D = 0$ and $C' \pm D' = 0$ respectively, which are integrable.

2.3. Symmetric models

In the DWIA we inevitably have a *post-prior* asymmetry. If there is an inherent asymmetry in the reaction, for example $Z_T \gg Z_P$, the choice between *post* and *prior* models can be argued in favour of one or the other. A detailed discussion of this question is given in the next section. A merit of the CDW theory is the intrinsic *post-prior* equivalence. Symmetry can be artificially introduced in our model by averaging the *post* and *prior* amplitudes. The resulting symmetrized DWIA is given by:

$$\tilde{a}_{fi}^{S}(\boldsymbol{\eta}) \equiv \tfrac{1}{2} \left[\tilde{a}_{fi}^{(-)}(\boldsymbol{\eta}) + \tilde{a}_{fi}^{(+)}(\boldsymbol{\eta}) \right] \tag{26}$$

Miraglia (1982) had also proposed making the impulse approximation in both entry and exit channels (generalized impulse approximation GIA). While it is much more difficult to calculate the GIA, it is not clear whether this GIA model will have a larger range of validity than the DWIA, and thus whether it offers a substantial gain in accuracy.

Table 2. Cross sections σ_{nl} (10^{-17}cm^2) of electron capture for helium nucleus-hydrogen collisions at energy E keV: $1s$ to nl transition. The integer in parenthesis indicates the power of ten by which the number has to be multiplied.

E(keV)		10	25	60	100	150	200
σ_{1s}	DWIA$_{post}$	2.76(0)	2.40(0)	9.02(-1)	4.87(-1)	2.42(-1)	1.25(-1)
	DWIA$_{prior}$	3.66(0)	4.22(0)	2.10(0)	8.58(-1)	3.24(-1)	1.41(-1)
	CDW	2.78(1)	3.07(0)	2.73(0)	1.10(0)	3.94(-1)	1.64(-1)
	SVCDW	2.92(-1)	9.93(-1)	1.70(0)	7.67(-1)	2.86(-1)	1.21(-1)
σ_{2s}	DWIA$_{post}$	2.07(1)	4.81(0)	1.30(0)	4.62(-1)	2.54(-1)	5.42(-2)
	DWIA$_{prior}$	1.77(1)	5.86(0)	1.33(0)	4.47(-1)	1.38(-1)	5.11(-2)
	CDW	1.68(2)	2.78(1)	3.53(0)	7.84(-1)	1.94(-1)	6.47(-2)
	SVCDW	1.58(1)	9.41(0)	1.90(0)	4.72(-1)	1.25(-1)	4.44(-2)
σ_{2p}	DWIA$_{post}$	1.05(2)	1.46(1)	2.26(0)	6.21(-1)	1.53(-1)	4.52(-2)
	DWIA$_{prior}$	1.32(2)	3.54(1)	5.79(0)	1.02(0)	1.93(-1)	5.20(-2)
	CDW	1.00(3)	1.10(2)	8.01(0)	1.23(0)	2.24(-1)	6.00(-2)
	SVCDW	6.07(1)	2.46(1)	2.95(0)	5.32(-1)	1.12(-1)	3.18(-2)

3. Results and discussion

We present results for capture cross sections as a function of energy and compare this data with experiment and other models. For the most part we use logarithmic graphs, but in addition we have compiled a small sample of the data in tabular form for reference purposes (tables 1 and 2). This helps to form detailed comparison of the *post* and *prior* forms of the DWIA results which would not be apparent from the graphs. We have used the CDW model as a benchmark (Belkić *et al* 1979) for the results. This model reproduces electron capture data very well over the high-energy range but suffers from a lack of unitarity at lower energies and invariably produces gross overestimates for capture at intermediate energies.

In figure 1 the DWIA results for electron capture cross sections of the $1s$-$2s$ transition in reaction (1) are shown. The corresponding data of Brown and Crothers (1996a) have not been presented, although they follow the experimental results very closely, even down to 10 keV/u. Instead our results are compared with experimental data and the continuum distorted-wave (CDW) results over the intermediate energy range: 20–250 keV/u. At the upper end of the energy regime we note that both DWIA curves merge with the CDW results. However this convergence is not uniform. If we refer to table 1 for energies beyond the scope of the graph, apart from noting the sharp fall in the size of the cross section (σ_{2s}), it is clear that at very high energies the *post* and *prior* results converge but begin to depart from the CDW data. This can be understood from noting

the importance of second-order effects at these energies. The CDW theory can partly but not fully account for these effects, and the DWIA data are more reliable estimates in this case. Nonetheless the CDW results are more than adequate for good estimates of cross sections at high energies.

The intermediate energy range covered by figure 1 indicates the disparity of these models more clearly. The CDW results continue rising sharply as is well-known (Belkić *et al* 1979). This is typical of the difficulties in applying high-energy perturbation theory over the intermediate energy range. We note that DWIA gives a slight improvement over CDW below around 50 keV/u, although its accord with experiment remains poor at lower energies. Furthermore the *post* and *prior* DWIA models show large differences below 50 keV/u. In common with the PWIA, the inherent *post-prior* asymmetry is expected to be greatest at the lowest velocities. As a general rule, the discrepancy is worse for PWIA than for DWIA (Ng and McCann 1997).

On theoretical grounds we can propose a prescription for the energy range of validity of the DWIA and for the preferred form (*post* or *prior*) of the theory in this particular reaction. Using the peaking criterion (McCann 1992), the orbital velocity of the electron in the final state is smaller than that in the initial state, and so one should apply CDW refinements in the exit channel and allow the PWIA to take account of momentum spread in the entrance channel. This implies that the *post* form should be preferred. Next, one can use the impulse hypothesis (Gravielle and Miraglia 1988) to establish the energy limit - given the largest orbital velocity is 1 a.u. the desired stipulation would be that $E \gg 25$ keV/u. This inequality is consistent with the experimental data in figure 1. Since we wish to know the practical limits of our model, the important question here is: how strong is the inequality? In this paper we aim to answer this question by a mixture of comparisons with experiment and other theories.

We have also computed, for the sake of completeness, several results using the symmetrized DWIA (equation 26). The results are shown in figure 1 and give the best agreement of all the calculations. Nonetheless this averaging procedure seems rather artificial to us, and the presence of a large *post-prior* discrepancy at the lower energies indicates that neither the *post* nor the *prior* form is very satisfactory around 25 keV/u. On the whole the theory of Brown and Crothers (1996a) still appears to be the most satisfactory description of the process both in physical and quantitative terms.

Figure 2 shows capture cross sections for $1s$-$2p$ transition. Below 40 keV/u, DWIA again gives slightly better results than CDW. In the high-energy range the results do not converge. Both sets of DWIA results differ and they in turn are lower than the CDW results by a fairly constant ratio (table 2). Again the *post* DWIA is expected to be the best physical model for this process and this is confirmed by the better agreement with the SVCDW of Brown and Crothers (1996a) over the energy range 20–100 keV/u. It has been noted that the experimental results all have systematic uncertainties with regard

to the normalization of the data. However these uncertainties are not large and a series of experiments has been carried out on this reaction process using independent estimates of the absolute magnitudes of the cross sections. It is very likely the experimental data in the figure are reliable both in terms of the energy dependence and absolute values. In any case we have not attempted to renormalize the data to theoretical predictions.

The process (1) is dominated by $1s$ and $2s$ transitions above 100 keV/u. For higher energies we can estimate capture into higher excited states (σ_n) by the rough approximation based on the n^{-3}-distribution of populations. The total cross section therefore becomes $\sigma_{total} = \sigma_1 + 1.62\sigma_2$ where σ_1 and σ_2 are cross sections of capture into the $n = 1$ and $n = 2$ levels respectively. Results for DWIA and CDW, in the energy range 125–2500 keV/u (figure 3), are very similar and are in good agreement with experimental data.

The proton-hydrogen collision calculations do not contain much *post-prior discrepancies* due to the nature of the charge exchange process being more or less symmetric. Their agreement with experimental data is very satisfactory. However the study of reaction (2) which has a strong in-built asymmetry would provide a much clearer critical assessment of DWIA. But first, the nature and implication of the asymmetry must be considered with care.

Generally in electron transfers from the ground state to one which is excited, an important point to consider is the momentum spread of the electron, before and after the collision. A sharply peaked momentum spread could be treated more efficiently by CDW with its peaking approximation. The impulse approximation should then be applied to the electronic state with the less sharply peaked momentum distribution. The momentum spread can be affected by the electron's distance from the nucleus and also by the magnitude of the nuclear charge, and is roughly of the order of $\sim Z/n$. Since the only asymmetry in proton-hydrogen collision comes from the difference in initial and final states and not from projectile and target nuclear charges, its *post-prior* discrepancies are not appreciable. The same, however, cannot be said for (2). In the forward reaction, we would expect an electron attached to the heavier (projectile) α–particle to have quite a broad momentum distribution. Since this situation arises after the collision, it would seem reasonable to use the *prior* form of DWIA. The *prior* form corresponds to a PWIA wavefunction in the exit channel, making the bare proton of the hydrogen atom more of a spectator particle than the helium nucleus. It has been argued (Gravielle and Miraglia 1991) that the converse should be true, the argument being based upon the idea of associating the impulse approximation with the stronger potential (*i.e.* in the entrance channel). We take the opposite viewpoint as the weight of evidence presented in this paper lends it sufficient support. Consequently for the time-reversed reaction (13), we apply inversion so that its *post* form becomes favourable.

Cross sections for selected energies for reaction (2) are tabulated in table 2, the

energy range (7–200 keV/u) being the same as that covered by figures 4 and 5. These show cross sections of capture into the $2s$ and $2p$ states. Comparison is made with the symmetrized variational continuum distorted-wave (SVCDW) method (Brown and Crothers 1996b), the conventional CDW theory and experimental results. In the case of the $2s$ transition DWIA fares rather poorly. While the curves follow the SVCDW curve at higher energies and avoids the low-energy divergence of the CDW, the agreement with experiment is not good over the important plateau region (figure 4). The DWIA completely fails to describe this feature. Results for the $2p$ transition (figure 5) on the other hand are less conclusive. The shortcomings of the DWIA around 50 keV/u for the $2s$ results could be attributed to the lack of strong coupling between the resonant states (H-$1s$, He^+-$2s, 2p$). Although the DWIA underestimates the $2s$ cross sections (figure 4) and overestimates the $2p$ results (figure 5), this can be explained by a second-order process involving the redistribution of populations: $H(1s) \rightarrow He^+(2p) \rightarrow He^+(2s)$. The inclusion of this effect in the SVCDW model brought good agreement with experiment. Its neglect in the DWIA means that there is a disconcerting gap between theory and experiment in figure 4, with a fraction of the cross section that should have gone towards the $2s$ transition ending up in the $2p$ instead.

The total cross section for capture into all states is shown in figure 6. The DWIA *prior* curve, with the n^{-3} scaling law included, performs remarkably well against both SVCDW and CDW. Major contribution to the total cross section comes from capture into the $2p$ state and DWIA models this quite well in its *prior* form, yielding good results. The use of the $1s$, $2s$, $2p$ results to extrapolate for capture to all states is doubtful, of course. A simple test shows that when the n^{-3} scaling law is applied to obtain CDW results for $\sigma_n \quad (n > 2)$, it underestimates the true CDW σ_n in the energy range 7–200 keV/u. This has the effect that the extrapolation can be in error by as much as 60% . In view of this, DWIA results for total cross sections should be considered as underestimates for capture to excited states and this could explain part of the shortfall between theory and experiment that we see in figure 6. If we were to assume that the underestimation for CDW will be of the same order of magnitude for DWIA at a fixed energy, appropriate augmentation of the results would bring them quite close to the experimental values.

4. Conclusions

In conclusion, despite its inherent *post-prior* discrepancies, DWIA can perform well even at energies as low as 20 keV/u if sufficient care is taken in choosing whether to use the *post* or *prior* form of the theory. This is very useful in establishing the energy range of validity. However the computational effort in evaluating DWIA is much greater than either CDW or PWIA model; hours as opposed to seconds on one of our RS/6000 workstations. The additional effort brings its reward in terms of better estimates of cross

sections towards the upper end of the intermediate energy range. This does provide very useful data for applications. There are awkward features of the calculation that make it difficult to compute without careful attention. However the method is significantly less expensive to compute than large-scale close-coupling methods, though it does not give the same accuracy or reliability over the intermediate energy regime. It is difficult to extend the DWIA method further. One might attempt a close-coupling approach akin to the SVCDW method. We take the view that significant improvements are difficult within the DWIA framework and that instead the SVCDW approach seems to combine the correct physical and mathematical features of the charge transfer processes in an elegant manner. This approach seems the most promising avenue for future work.

Acknowledgments

We are grateful to the UK Engineering and Physical Sciences Research Council for their support of this work through a research studentship and provision of computing resources. The EPSRC-funded Durham/Newcastle Atmol cluster was used along with the Columbus workstation cluster at Rutherford-Appleton Laboratory. We are grateful to Dr Geoff Brown for providing us with numerical data for the SVCDW results for α–particle collisions, and for useful discussions on this subject.

References

Appell P and Kampé de Feriet J 1926 *Fonctions Hypergéometriques et Hypersphériques* (Paris: Gauthier-Villars)

Barnett C F 1990 *Oak Ridge National Laboratory* Report No 6086 (unpublished)

Belkić Dz, Gayet R and Salin A 1979 *Phys. Rep.* **56** 279.

Bransden B H and McDowell M R C 1992 *Charge Exchange and the Theory of Ion-Atom Collisions (Oxford: Oxford Science Publications)*

Brown G J N and Crothers D S F 1994 *J.Phys. B: At. Mol. Opt. Phys.* **27** 5309.

——1996a *Phys. Rev. Lett.* **76** 392 2

——1996b *J.Phys. B: At. Mol. Opt. Phys.* **29** L705

Ćirić D, Dijkkamp D, Vlieg E and de Heer F J 1985 *J. Phys. B: At. Mol. Opt. Phys.* **18** L17

Coleman J P and Trelease S 1968 *Proc. R. Soc.* **85** 1097

Fritsch W and Lin C D 1991 *Phys. Rep.* **202** 1

Gilbody H B and Ryding G 1966 *Proc. R. Soc. (London)* **A291** 438

Gilbody H B 1995 *XIX ICPEAC Invited Papers, British Columbia, Canada, Edited by L J Dubé, J B A Mitchell, J W McConkey and C E Brion (AIP Press: New York)* **360** 19

Gravielle M S and Miraglia J E 1988 *Phys. Rev.* A **38** 5034

——1991 *Phys. Rev.* A **44** 7299

Jakubassa-Amundsen D H and Amundsen P 1980 *Z. Phys.* A **297** 203

Janev R K, Langer W D, Evans Jr. K and Post Jr. D E 1987 *Elementary Processes in Hydrogen-Helium Plasmas (Berlin and New York: Springer-Verlag)*

Kuang Y and Lin C D 1996 *J. Phys. B: At. Mol. Opt. Phys.* **29** 1027
McCann J F 1992 *J.Phys. B: At. Mol. Opt. Phys.* **25** 449
McLaughlin B M, Winter T G and McCann J F 1997 *J. Phys. B: At. Mol. Opt. Phys.* **30** 1043.
Miraglia J E (1982) *J. Phys. B: At. Mol. Phys.* **15** 4205.
Morgan T J, Stone J and Mayo R 1980 *Phys. Rev.* **A22** 1460
Ng Y H and McCann J F 1997 (in preparation)
Olsson P O M 1964 *J. Math. Phys.* **5** 420
Schwab W, Baptista G B, Justiniano E, Schuch R, Vogt H and Weber E W 1987 *J. Phys. B: At. Mol. Opt. Phys.* **20** 2825
Shah M B and Gilbody H B 1978 *J.Phys. B: At. Mol. Opt. Phys.* **11** 121
Slim H A and Ermolaev A M 1994 *J.Phys. B: At. Mol. Opt. Phys.* **27** L203
Van Zyl B 1993 *XVIII ICPEAC Invited Papers, Aarhus, Denmark, Edited by T Anderson, B Fastrup, F Folkmann, H Knudsen and N Andersen (AIP Press: New York)* **295** 684
Toburen L H, Nakai M Y and Langley R A 1968 *Phys. Rev.* **171** 114

Figure Captions

- Figure 1: Cross sections for $1s \rightarrow 2s$ capture for process (1): DWIA(*prior*) (——), DWIA(*post*) (- - - -), symmetrized DWIA ($\diamond$), CDW ($\cdot\cdot\cdot\cdot\cdot\cdot$) and experimental results by Morgan *et al* (1980) ($\bullet$).
- Figure 2: Cross sections for $1s \rightarrow 2p$ electron capture for process (1): DWIA(*prior*) (——), DWIA(*post*) (- - - -), CDW ($\cdot\cdot\cdot\cdot\cdot\cdot$) and experimental results by Barnett (1990) ($\bullet$).
- Figure 3: Total cross section of electron capture into all states in collisions between proton and hydrogen: DWIA (——), CDW ($\cdot\cdot\cdot\cdot\cdot\cdot$) and experimental results by Toburen *et al* (1968) ($\bullet$), Gilbody and Ryding (1966) ($\triangle$) and Schwab *et al* (1987) ($\square$).
- Figure 4: Cross sections for $1s \rightarrow 2s$ electron capture for process (2): DWIA(*prior*) (——), DWIA(*post*) (- - - -), CDW ($\cdot\cdot\cdot\cdot\cdot\cdot$), SVCDW (— $\cdot$ —) and experimental results by Shah and Gilbody (1978) ($\bullet$).
- Figure 5: Cross sections for $1s \rightarrow 2p$ capture for process (1): DWIA(*prior*) (——), DWIA(*post*) (- - - -), CDW ($\cdot\cdot\cdot\cdot\cdot\cdot$), SVCDW (— $\cdot$ —) and experimental results by Ćirić *et al* (1985) ($\bullet$).
- Figure 6: Total cross section of electron capture into all states in Collisions between helium nuclei and hydrogen: DWIA(*prior*) (——), DWIA(*post*) (- - - -), CDW ($\cdot\cdot\cdot\cdot\cdot\cdot$), SVCDW (— $\cdot$ —) and experimental results by Shah and Gilbody (1978) ($\bullet$).

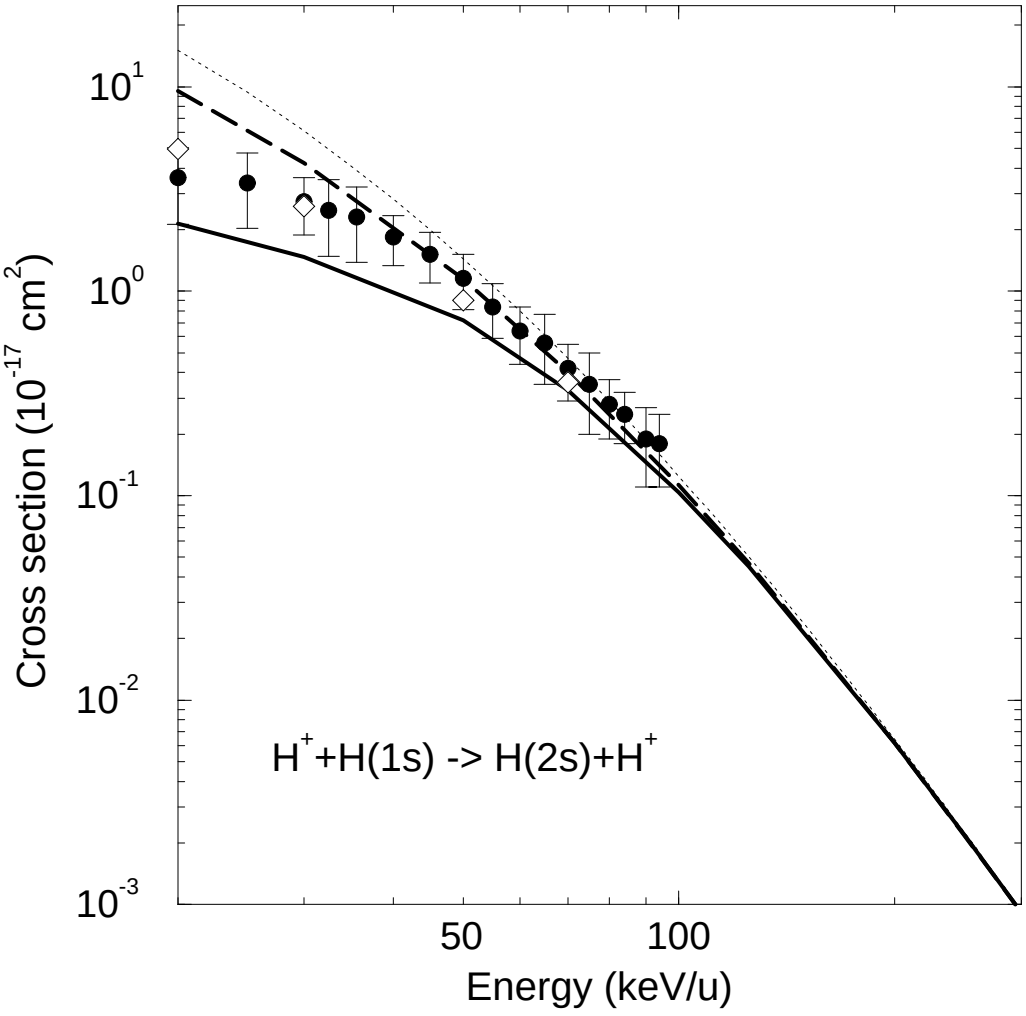
Cross section (10^{-17} cm^2)
10^1
10^0
10^{-1}
10^{-2}
10^{-3}
50
100
Energy (keV/u)
H^++H(1s) -> H(2s)+H^+

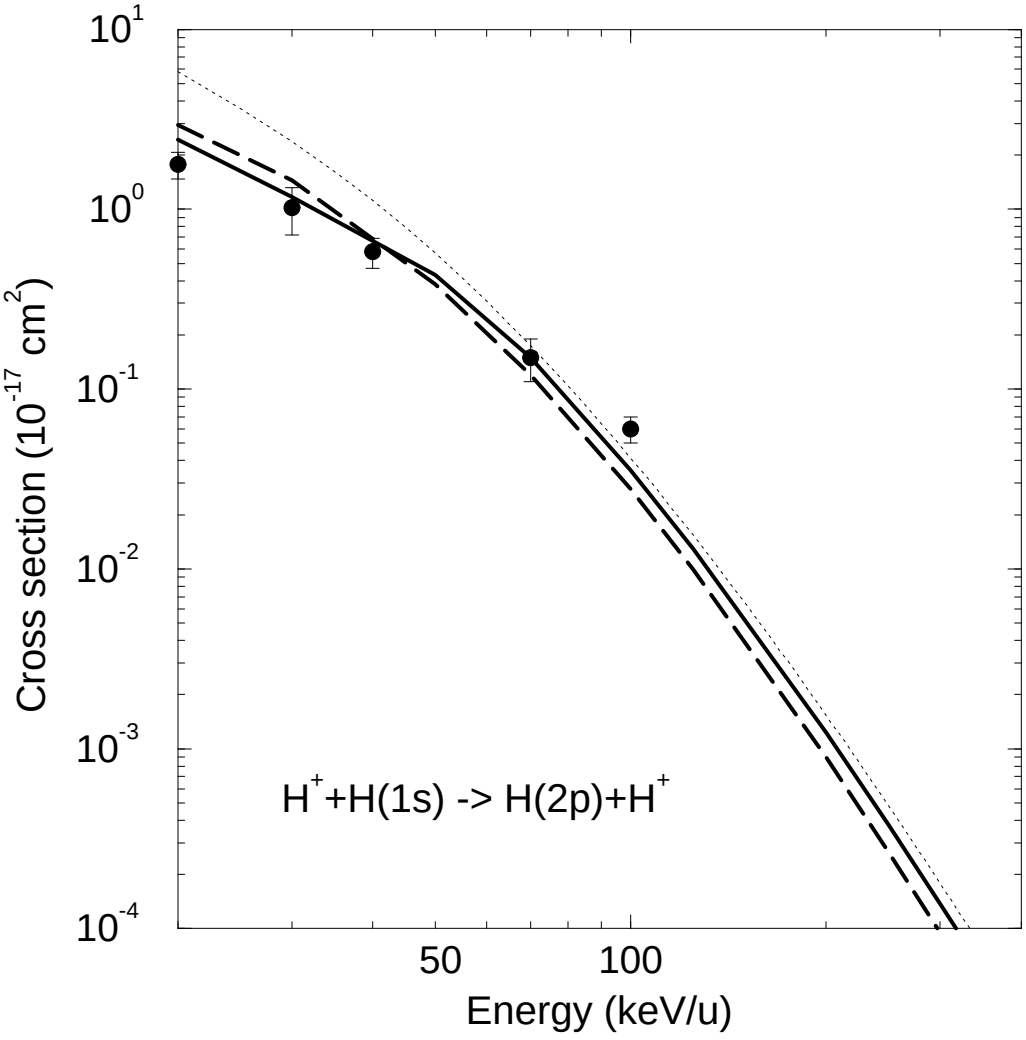
Cross section (10^{-17} cm^2)
10^1
10^0
10^{-1}
10^{-2}
10^{-3}
10^{-4}
50
100
Energy (keV/u)
H^++H(1s) -> H(2p)+H^+

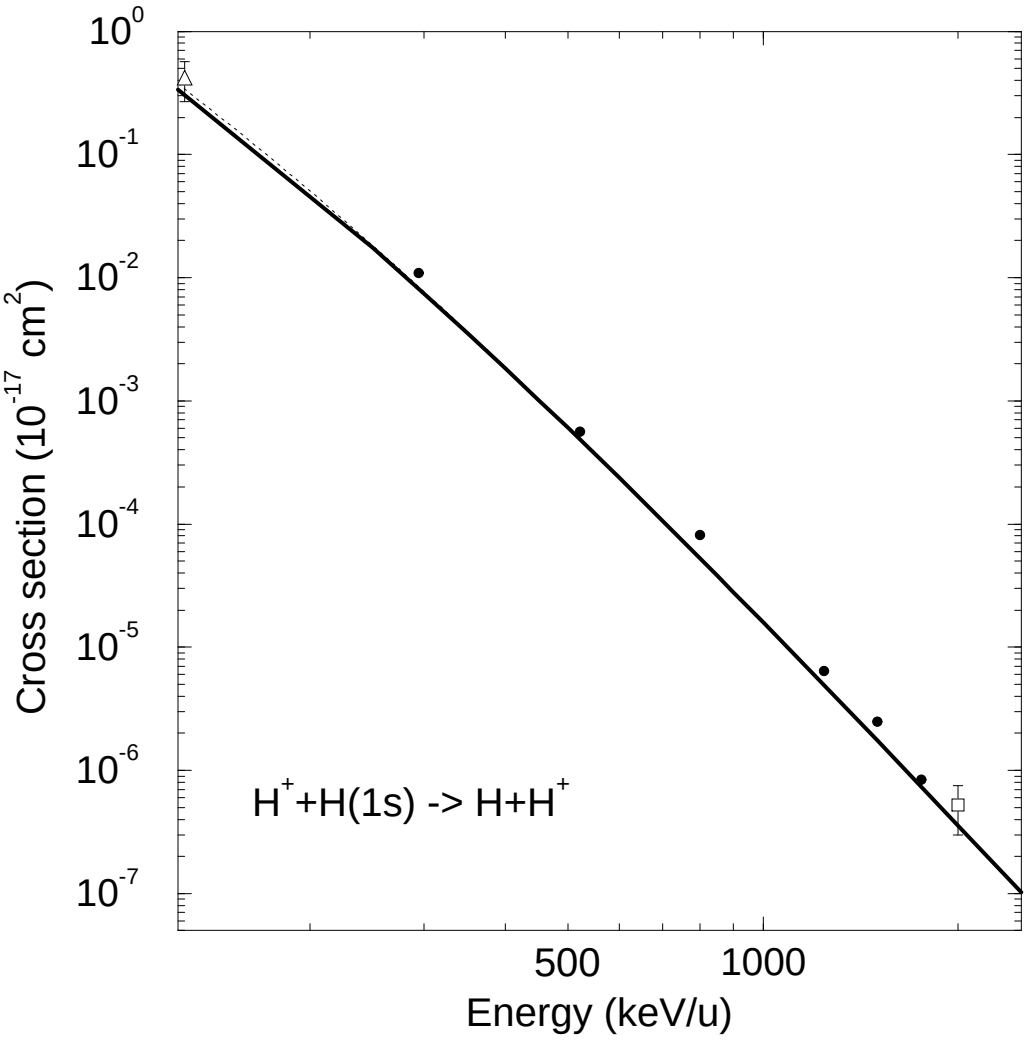
Cross section (10^{-17} cm^2)
10^0
10^{-1}
10^{-2}
10^{-3}
10^{-4}
10^{-5}
10^{-6}
10^{-7}
500
1000
Energy (keV/u)
H^++H(1s) -> H+H^+

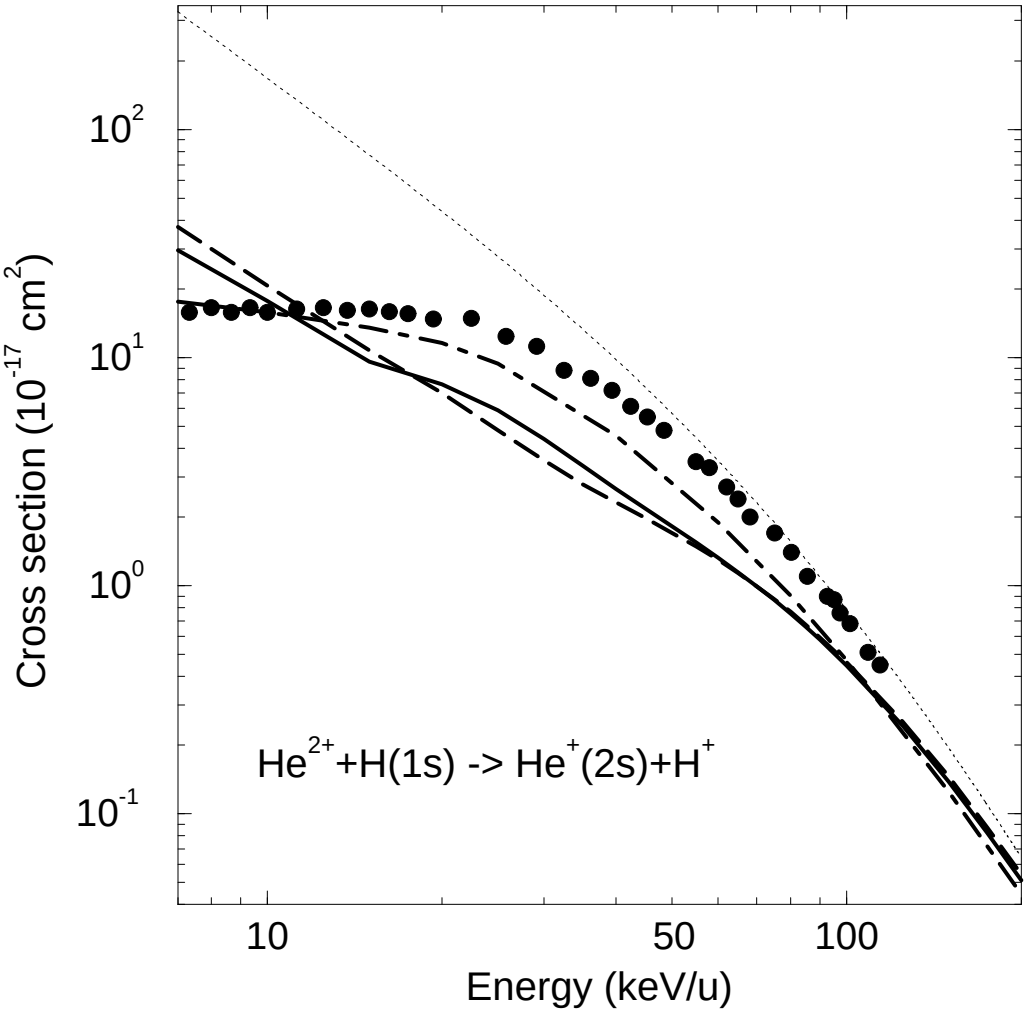
Cross section (10^{-17} cm^2)
10^2
10^1
10^0
10^{-1}
10
50
100
Energy (keV/u)
He^{2+}+H(1s) -> He^+(2s)+H^+

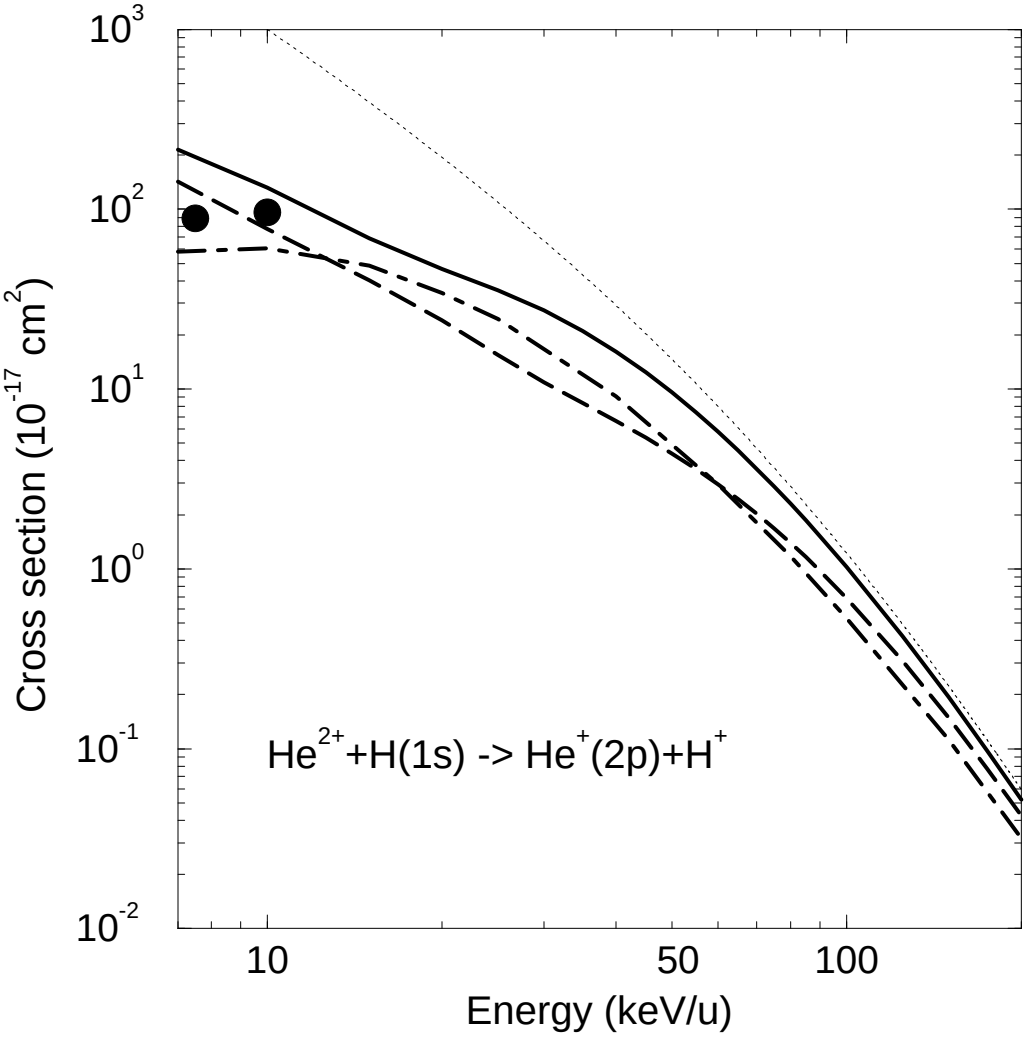
Cross section (10^{-17} cm^2)
10^3
10^2
10^1
10^0
10^{-1}
10^{-2}
10
50
100
Energy (keV/u)
He^{2+}+H(1s) -> He^+(2p)+H^+

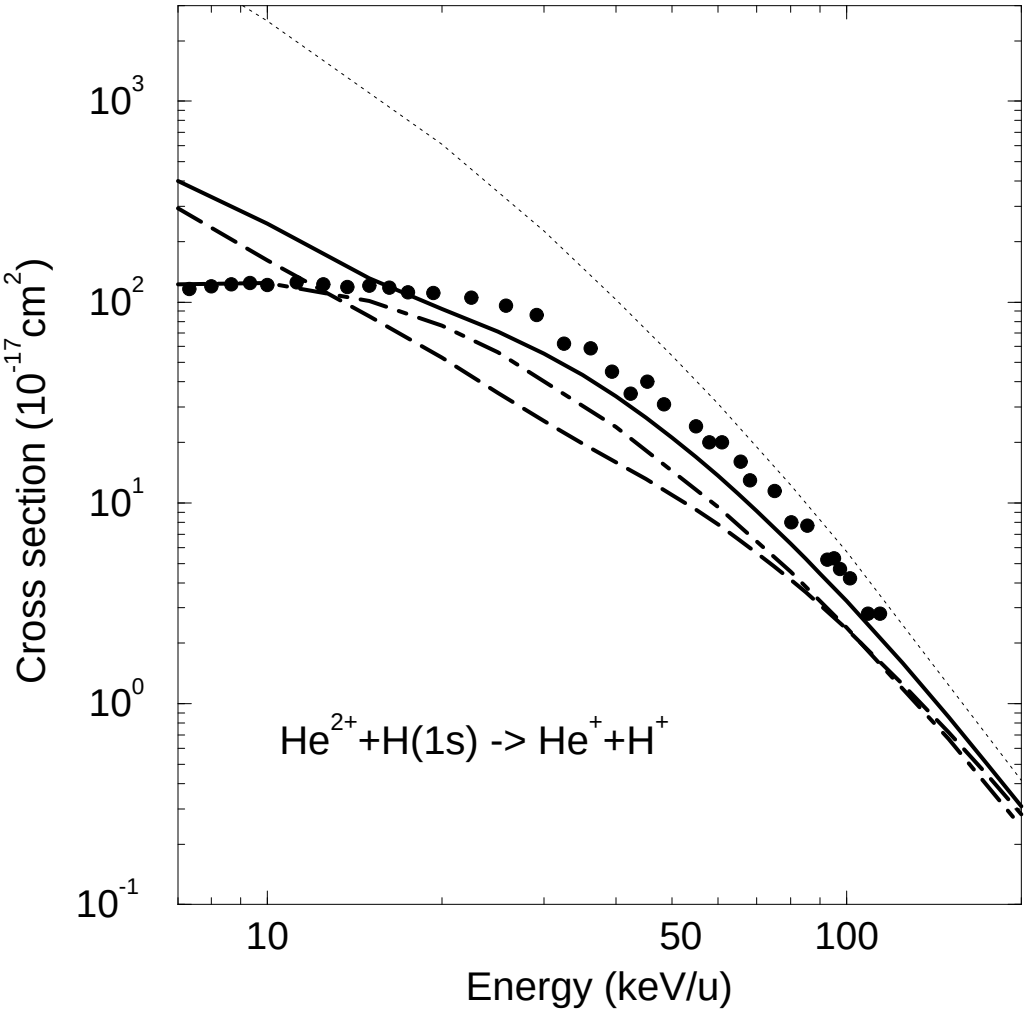
Cross section (10^{-17}cm^2)
10^3
10^2
10^1
10^0
10^{-1}
10
50
100
Energy (keV/u)
He^{2+}+H(1s) -> He^++H^+